Electronic Supplementary Material (ESI) for Journal of Materials Chemistry C.
This journal is © The Royal Society of Chemistry 2023

Supplementary Information

Tunable optical properties of transition metal dichalcogenide nanoparticles synthesized by femtosecond laser ablation and fragmentation

Anton S. Chernikov,[a] Gleb I. Tselikov,[b,c] Mikhail Yu. Gubin,*[b,a] Alexander V. Shesterikov,[b,a] Kirill S. Khorkov,[a] Alexander V. Syuy,[b,c] Georgy A. Ermolaev,[b,c] Ivan S. Kazantsev,[b,c] Roman I. Romanov,[d] Andrey M. Markeev,[b] Anton A. Popov,[d] Gleb V. Tikhonowski,[c,d] Olesya O. Kapitanova,[b,e] Dmitry A. Kochuev,[a] Andrey Yu. Leksin,[a] Daniil I. Tselikov,[d] Aleksey V. Arsenin,[b,c,f] Andrei V. Kabashin,[g] Valentyn S. Volkov,[c] and Alexei V. Prokhorov,[b,a]

[a]*Department of Physics and Applied Mathematics, Vladimir State University named after A. G. and N. G. Stoletovs (VlSU), Vladimir 600000, Russia*
[b]*Center for Photonics and 2D Materials, Moscow Institute of Physics and Technology, Dolgoprudny 141701, Russia, E-mail: myugubin@gmail.com*
[c]*Emerging Technologies Research Center, XPANCEO, Dubai Investment Park First, Dubai, UAE*
[d]*National Research Nuclear University MEPhI, Moscow 115409, Russia*
[e]*Faculty of Chemistry, Lomonosov Moscow State University, Moscow 119991, Russia*
[f]*Laboratory of Advanced Functional Materials, Yerevan State University, Yerevan 0025, Armenia*
[g]*CNRS, LP3, Aix-Marseille Université, Marseille 13288, France*

S1. Measured zeta potential for synthesized nanoparticles.

The stability of the synthesized NPs can be evaluated, for example, by measuring their zeta potential distribution. NPs can be considered as stable if the absolute value of zeta potential is near 30 mV [1,2]. Figure S1 shows the zeta potential distribution measured for the MoS_2 nanoparticles obtained by laser ablation in ethanol. This distribution for MoS_2 NPs has a maximum at –34 mV suggesting their stability [1,2].

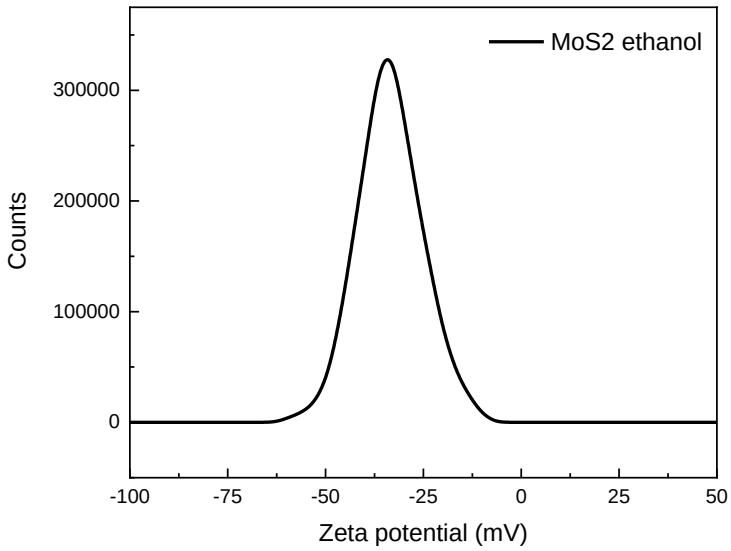

Figure S1. Zeta potential distribution for MoS_2 nanoparticles synthesized by laser ablation in ethanol.

S2. Lattice spacing for hybrid NP synthesized in ethanol.

Figure S2 shows a HR-TEM image of NP synthesized after laser ablation followed by laser fragmentation. One can see that NPs consist of small fragments of layered materials with random orientation of the layers relative to each other. The estimation of lattice spacing shows the existence of both MoS_2 and MoO_{3-x} phases at once in one NP. The lattice spacing for MoO_{3-x} material approximately takes the values within the range 0.2–0.4 nm depending on the x and different planes of α-MoO_3 [3–7] that is approximately 2–2.5 times less than for MoS_2 [8–10] (lattice spacing approximately equals to 0.65 nm). Despite the fact that TEM has a high resolution, it is rather difficult to detect MoO_{3-x} layers in NPs, because they consist of small fragments of layered materials arranged randomly and have quite a large size. As a result, MoO_{3-x} layers can be identified by the TEM method only at the NP edge when the electron beam passes through NP along a short chord.

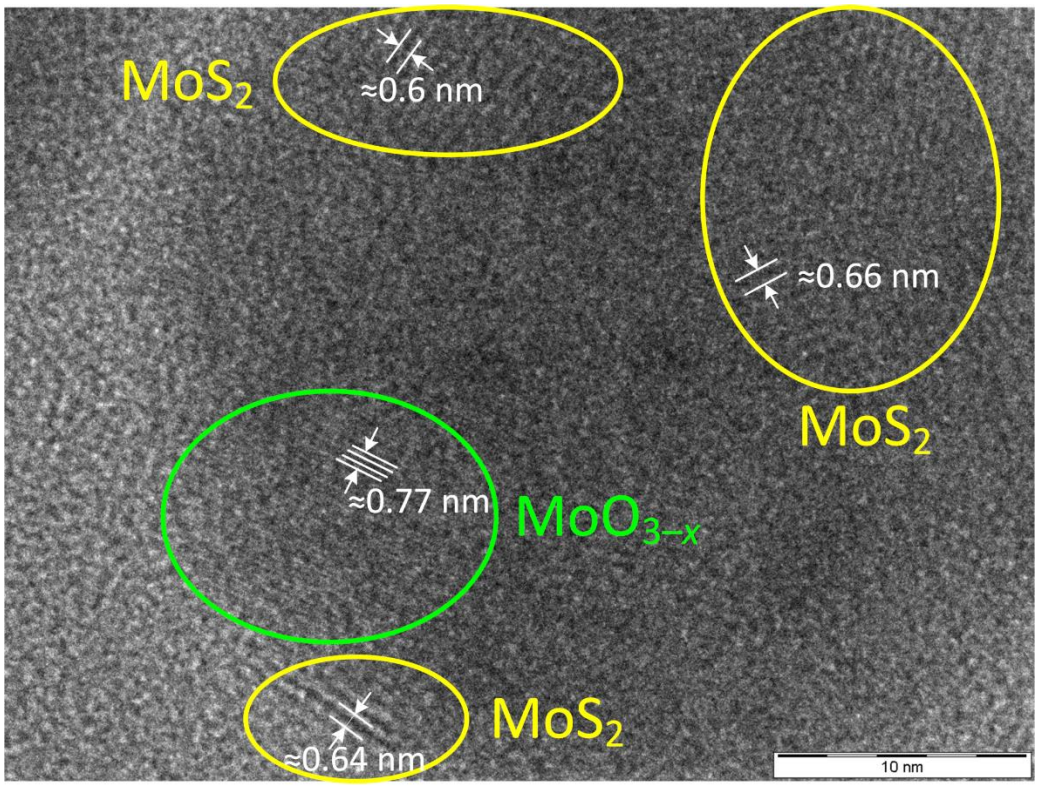

Figure S2. HR-TEM image of NP from the solution obtained after laser ablation followed by laser fragmentation in ethanol with depicted lattice spacing for MoS_2 and MoO_{3-x} materials.

S3. XPS analysis of compositions obtained after laser ablation/fragmentation.

The additional analysis of XPS spectra of solutions was carried out to identify the stable chemical compounds that appear after laser ablation and fragmentation processes.

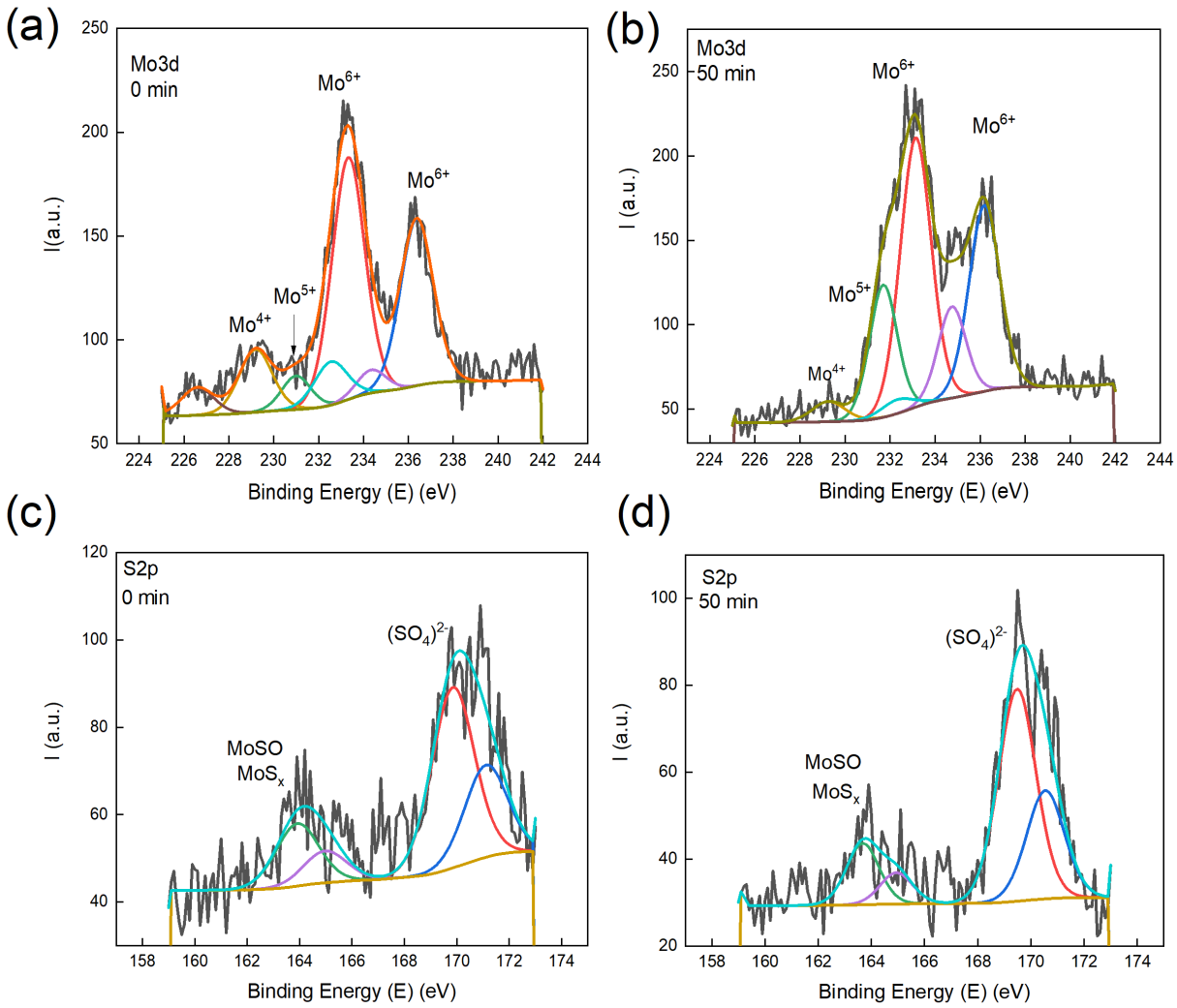

Figure S3. (a) Mo3d XPS spectra of ablated in ethanol MoS_2 NPs, (b) fragmented at 50 minutes in ethanol $MoSO_x$ NPs. (c) S2p XPS spectra of ablated in ethanol MoS_2 NPs, (d) fragmented at 50 minutes in ethanol $MoSO_x$ NPs. Decomposition of Mo3d (a,b) and S2p (c,d) core level signals into their constituents.

Figure S3 demonstrates Mo3d and S2p XPS spectra of ablated in ethanol MoS_2 NPs and fragmented at 50 minutes $MoSO_x$ NPs. For Mo3d spectra the peak at 229.3 eV corresponds to Mo^{4+} state (MoS_2), 231.5 eV to Mo^{5+} and 232.9 eV to Mo^{6+} state (MoO_3). Also, the peak at 226 eV corresponds to S2s line. For S2p spectra, the peak at 163.5 eV corresponds to sulfur in MoS_x and MoSO compounds while the peak at 169 eV corresponds to sulfate $(SO_4)^{2-}$ formation. The relative concentration of these states is given in Table S1.

Table S1. Composition of laser-synthesized MoS_x nanoparticles based on the decomposition of Mo3d, S2p and O1s peaks.

0 min							
Name	State assigned	Peak	Height	FWHM	Area (P)	Atomic	Q
		BE	CPS	eV	CPS.eV	%	
S2p3_315916 2s B	MoS_x, MoSO	163,91	14,3	1,92	29,81	4,31	v
S2p3_315916 2s Å	$(SO_4)^{2-}$	169,85	41,37	192	36,20	12,48	v
S2p1_315916 2s B		164,97	731	1,92	15,23	0,00	
S2p1_315916 2s Å		171,11	21,13	1,92	43,48	0,00	
O1s_315916 2s D		535,5	81,91	1,63	144,33	8,54	v

O1s_315916 2s C		532,5	115,04	1,92	239,74	14,17	v
O1s_315916 2s B		533,82	343,39	1,92	715,62	42,32	v
O1s_315916 2s Å		531,08	76,52	1,92	159,47	9,42	v
Mo3d_3159_16_2s D		226,6	13,32	1,73	24,54	0,00	
Mo3d5_3159_16_2s C	MoS_2	229,19	30,38	1,73	56,98	1,65	v
Mo3d5_3159_16_2s B	MoS_x	231	16,19	1,53	26,90	0,78	v
Mo3d5_3159_16_2s A	MoO_3	233,33	116,72	1,73	218,92	6,33	v
Mo3d3_3159_16_2s C		232,54	20,97	1,73	39,34	0,00	
Mo3d3_3159_16_2s B		234,35	11,18	1,53	18,57	0,00	
Mo3d3_3159_16_2s A		236,38	80,58	1,73	151,14	0,00	
20 min							
Name	State assigned	Peak	Height	FWHM	Area(P)	Atomic	Q
		BE	CPS	eV	CPS,eV	%	
S2p3_3159.15 B	MoS_x, MoSO	164	13,09	1,44	20,47	1,94	v
S2p3_3159.15 A	$(SO_4)^{2-}$	168,96	47,25	1,49	76,13	7,21	v
S2p1_3159.15 B		165,26	6,69	1,44	10,45	0	
S2p1_3159_15 A		170,2	24,13	1,49	38,89	0	
O1s_3159.15C		533,21	199,14	1,38	406,16	15,7	v
O1s_3159.15 8		532,1	497,69	1,4	755,74	29,21	v
O1s_3159.15 A		530,88	503,77	1,43	778,11	30,06	v
Mo3d_3159_15 D		226,42	13,1	2,12	30,02	0	
Mo3d5_3159_15 C	MoS_2	228,88	31,76	1,73	59,57	1,13	v
Mo3d5_3159 15 B	MoS_x	231,5	114,86	134	167,16	3,16	v
Mo3d5_3159 15 A	MoO_3	232,95	369,06	154	613,91	11,61	v
Mo3d3.315915C		232,11	21,93	1,73	41,13	0	
Mo3d3.3159_15 B		234,55	79,3	134	115,41	0	
Mo3d3.3159_15 Å		260	254,8	154	423,84	0	
30 min							
Name	State assigned	Peak	Height	FWHM	Area(P)	Atomic	Q
		BE	CS	eV	CPS.eV	%	
S2p3_3159.17 B	MoS_x, MoSO	163,68	14,14	144	22,11	3,01	v
S2p3_315917 Å	$(SO_4)^{2-}$	169,49	48,83	167	88,39	12,04	v
S2p1_3159.17 B		164,94	7,22	1,44	11,29	0,00	
S2p1_315917 Å		17055	2494	1,67	45,13	0,00	
O1s_3159.17 D		535,16	41,38	1,44	64,67	3,60	v
O1s_3159.17 C		533,62	337,82	1,41	515,9	28,69	v
O1s_3159.17 B		532,39	245,85	1,29	343,43	19,09	v
O1s_315917 Å		531,06	233,09	1,57	395,7	21,99	v
Mo3d5_3159.17 C	MoS_2	229,27	11,97	1,73	22,45	0,61	v
Mo3d5_3159_17 B	MoS_x	231,70	78,43	1,46	123,85	3,37	v
Mo3d5_3159_17 A	MoO_3	233,13	159,66	1,62	279,49	7,60	v
Mo3d3_3159_17C		232,32	8,26	1,73	15,5	0,00	
Mo3d3_3159_17 B		234,75	54,15	1,46	85,51	0,00	
Mo3d3_3159_17 A		236,18	110,23	1,62	192,95	0,00	
50 min							
Name	State assigned	Peak	Height	FWHM	Area(P)	Atomic	Q
		BE	CPS	eV	CPS.eV	%	
S2p3_3159.18 B	MoS_x, MoSO	163,56	16,55	1,92	34,50	3,21	v
S2p3_3159.18 Å	$(SO_4)^{2-}$	168,85	39,37	1,83	77,88	7,25	v
S2p1_3159.18 B		164,62	846	1,92	17,62	0,00	
S2p1_3159.18 Å		170,11	20,11	1,83	39,77	0,00	
O1s_3159_18 C		533,61	160,11	1,92	333,67	12,69	v
O1s_3159_18 B		532,05	521,11	1,9	1071,30	40,72	v
O1s_315918 A		530,77	365,72	1,37	542,50	20,61	v

Mo3d5_3159_18 C	MoS_2	229,31	30,54	1,73	57,25	1,06	v
Mo3d5_3159_18 B	MoS_x	231,50	124,01	1,21	162,62	3,02	v
Mo3d5_3159_18 A	MoO_3	232,93	328,01	1,73	615,18	11,44	v
Mo3d3_3159_18 C		232,66	21,09	1,73	39,53	0,00	
Mo3d3_3159_18 B		234,71	85,61	1,21	112,27	0,00	
Mo3d3_3159_18 A		236,07	226,45	1,73	424,72	0,00	

References

1. R. Choudhary, D. Khurana, A. Kumar and S. Subudhi, J. Exp. Nanosci. 2017, 12, 140–151.
2. A. Kumar, C.K. Dixit, Advances in Nanomedicine for the Delivery of Therapeutic Nucleic Acids. 2017, 43–58.
3. S. Duraisamy, A. Ganguly, P. K. Sharma, J. Benson, J. Davis and P. Papakonstantinou, ACS Appl. Nano Mater. 2021, 4, 2642–2656.
4. B. B.Wang, X. X. Zhong, B. M. Ming, M. K. Zhu, Y. A. Chen, U. Cvelbar, K. Ostrikov, Appl. Surf. Sci. 2019, 480, 1054–1062.
5. X. Lu, R. Wang, F. Yang, W. Jiao, W. Liu, L. Hao and X. He, J. Mater. Chem. C, 2016, 4, 6720-6726.
6. S. Balendhran, J. Deng, J. Z. Ou, S. Walia, J. Scott, J. Tang, K. L. Wang, M. R. Field, S. Russo, S. Zhuiykov, M. S. Strano, N. Medhekar, S. Sriram, M. Bhaskaran and K. Kalantar-zadeh, Adv. Mater. 2013, 25, 109-114.
7. M. Dieterle, G. Weinberg and G. Mestl, Phys. Chem. Chem. Phys., 2002,4, 812-821.
8. G. I. Tselikov, G. A. Ermolaev, A. A. Popov, G. V. Tikhonowski, D. A. Panova, A. S. Taradin, A. A. Vyshnevyy, A. V. Syuy, S. M. Klimentov, S. M. Novikov, A. B. Evlyukhin, A. V. Kabashin, A. V. Arsenin, K. S. Novoselov and V. S. Volkov, PNAS 2022, 119, e2208830119.
9. X. Li and H. Zhu, J. Materiomics, 2015, 1, 33–44.
10. Y. Zhao and G. Ouyang, Sci. Rep., 2019, 9, 17381.